Heliyon 9 (2023) e16428

Contents lists available at ScienceDirect

Heliyon

journal homepage: www.cell.com/heliyon

Research article

Optimized design and experimental validation of sound absorption coefficient performance in aluminium metal foam by spark plasma sintering

Mohammad Javad Jafari [a], Rohollah Fallah Madvari [a,b,*], Touradj Ebadzadeh [c]

[a] Department of Occupational Health and Safety Engineering, School of Public Health and Safety, Shahid Beheshti University of Medical Sciences, Tehran, Iran
[b] Department of Occupational Health Engineering, School of Public Health, Shahid Sadoughi University of Medical Sciences, Yazd, Iran
[c] Department of Ceramic, Materials and Energy Research Center, Karaj, Iran

ARTICLE INFO

Keywords:
Sound absorption coefficient (SAC)
Metal foam
Optimization
Acoustic model
Spark plasma sintering (SPS)

ABSTRACT

Determining the structural properties of aluminum metal foam is essential to predicting its acoustic behavior. Acoustic models are presented that show the relationship between the morphology of the absorber and the sound absorption coefficient (SAC). Optimizing the parameters affecting the SAC can be the maximum theoretically SAC achieved at each frequency. In the previous article (https://doi.org/10.32604/sv.2021.09729) the parameters of porosity percentage (Ω), pore size (D) and pore opening size (d) were optimized by the genetic algorithm and Lu model. In this study, the optimal aluminum metal foam was synthesized using Spark Plasma Sintering (SPS), with the maximum temperature of 420 °C and final pressure of 20 MPa in samples with thicknesses of 5, 10, 15 and 20 mm in different frequencies from 1000 to 6300 Hz. The crystal structure and microstructure of samples were investigated using XRD and SEM. Optimized metal foam SAC (0.67, 0.9, 1 and 1) and experimental peak SAC (0.44, 0.67, 0.76 and 0.82) were compared with the optimized SAC in 5, 10, 15 and 20 mm thicknesses, respectively. The values of the coefficient of determination (R^2) according to multiple linear regression (MLR) for the two optimized SAC and experimental in thicknesses of 5, 10, 15 and 20 mm were 0.90, 0.95, 0.96 and 0.90, respectively. The results of this study show that porous metal foam can have a high absorption coefficient in any desired thickness and frequency by using the optimal morphology.

1. Introduction

Criteria for evaluating the effectiveness of sound absorbers such as metal foam are expressed by the sound absorption coefficient (SAC). One of the research activities in the field of noise control is to obtain an absorber sample that has high sound absorption in the desired and discrete (specific) frequency. Determining, modifying and optimizing the SAC absorbers have a major role in sound design

Abbreviations: Ω, porosity percentage; D, pore size; d, pore opening size; SAC, Sound Absorption Coefficient; SPS, Spark Plasma Sintering; COD, coefficient of determination.

* Corresponding author. Department of Occupational Health Engineering, School of Public Health, Shahid Sadoughi University of Medical Sciences, Yazd, Iran.
E-mail addresses: Fallah134@gmail.com, R.fallahmadvari@ssu.ac.ir (R.F. Madvari).

https://doi.org/10.1016/j.heliyon.2023.e16428
Received 19 December 2022; Received in revised form 14 May 2023; Accepted 16 May 2023
Available online 24 May 2023

and control [1,2]. Adjusting the microscopic geometry of the absorbers plays an important role in optimizing the performance and obtaining the appropriate sound absorption spectrum. Proper selection of pores connected in a porous environment can help improve sound absorption performance.

According to the researches, many factors such as porosity percentage (Ω), pore size (D), pore opening size (d), thickness and structure of the pore (open or closed) have an effective role in sound absorption behavior due to their significant effect on the air flow resistance of foams [3–7]. Therefore, it seems that changing the microstructure of foams leads to improve the SAC in them. In this regard, the (Ω), (D) and (d) of the foam are of special importance in sound absorption.

So far, various researchers have made metal foams in different Ω and D and reported the best SAC of them [3,8–10]. Since, the sounds are different in the frequency in industries (especially discrete frequency), therefore the results of the above studies in each industry must be repeated through trial and error to make the appropriate absorbing properties that require cost and time. To solve these problems, one should look for a solution that can be used to determine the appropriate absorber characteristics through acoustic models and computer optimization with sound properties, and then makes the absorber.

In Lu model [11], it emphasizes on revealing the correlation between sound absorption and morphological parameters such as (Ω), (D), and (d), and several studies have obtained good agreement between theoretical and experimental conditions [3,8–10].

In metal foam absorbers to have specific sound properties, the appropriate type and size of pores can be obtained by using sound models for optimal absorption at any given frequency. Computer tools such as optimization algorithms (Genetic, PSO, local search, etc) are needed to optimize the parameters affecting the SAC of these models [12,13]. Optimization algorithms are descriptions of steps that are properly implemented in a computer program to find an approximation of an optimal point. Approximate algorithms such as genetic metaheuristic are among these optimization tools that can obtain appropriate (near-optimal) optimization problems in a short time [14]. After the theoretically optimal parameters have been obtained, the foam is produced.

The liquid-state processing techniques, solid-phase processing (SPP), solid-phase precipitation, and others are currently methods for making aluminum metal foams used in the commercial production of porous metals [15–17]. However, it is difficult to control pore properties such as (Ω), (D) and pore morphology. To improve the mechanical and other properties of aluminum foam, it is necessary to control the pore morphology [18].

In the last few decades, powder metallurgy (PM), a new processing route with high mechanical performance, has attracted much attention from researchers and industrialists [19]. Hot isostatic pressing, hot extrusion and spark plasma sintering (SPS) are different methods of powder metallurgy [19]. The main advantage of the SPS technique is a nano-microstructure controlled sintering method [20]. The SPS process has other advantages, such as (I) high thermo-efficiency (II) spontaneous heating (III) better self (IV) fast sintering under low temperatures [21].

The SPS method has the ability to more fully densify materials at a lower temperature, processing time, and with less grain growth [22]. Also, this technique could remove the alumina oxide layer on the surface of the aluminum particles and improves the sinterability of the particles.

According to the type of acoustic model, the conditions of optimization and controlled production of foam, which were described above, metal foam was prepared by Spacer and SPS methods [23,24]. This process consists of four steps: mixing, pressing, sintering and leaching. In the sintering method, by changing the weight percentage of aluminum, salt and the size of the salt powder, the Ω, D and the d can be obtained according to the optimization results.

If we can determine the optimum (Ω), (D), and (d) of metal foams for absorbing a specific frequency sound or a certain amount of absorption and then make the foam, we have taken an important step in making the conscious construction of porous foams. Due to the importance of the subject of this study, an attempt has been made to theoretically determine the optimal parameters of metal foam using the method of genetic metaheuristic algorithm and sound absorption models. Then, the construction of metal foams was done based on the measurements and optimum parameters.

2. Experimental procedures

2.1. Optimization

In the previous study (https://doi.org/10.32604/sv.2021.09729) [25], at first, the models of sound propagation in the porous absorbers of metal foams was investigated and according to the objectives and possibilities, the Lu model was selected. Using a genetic algorithm, the parameters affecting the SAC such as Ω, D and d of the pore were optimized. Therefore, at firat the formulas of Lu theory [11] were coded in MATLAB software and then validation was done using the Benchmarking method. The benchmarking method was used to compare the coded results with the coded results in the Lu article. According to the results obtained, there was a good agreement between the coding of the results of the Lu model [25]. The optimization of genetic algorithm was performed using competition method (tournament) by selecting members to produce offspring and applying mutations. Population equal to 50; Generation percentage 80%; Mutation percentage 30%; The mutation rate was set to 0.02 and the number of replicates to 150. Also, the Uniform Crossover method was used for the generation process [25].

2.2. Spark plasma sintering (SPS)

In this research, aluminum powder and commercial NaCl (spherical shape) from Merck with a purity of more than 99% were used as raw materials (Table 1). After preparing After preparing the appropriate raw materials, X-ray diffraction (XRD, PW3710 model made by Philips, the Netherlands) of these powders was taken to ensure their quality. By examining the patterns and comparing them

with X-ray diffraction reference cards related to these materials in High Score Plus software, analysis of raw materials was performed.

The size of the salt particles was determined based on the required (D). Because salts with the desired dimensions were not found in the market, the process of crushing and sieving was used to prepare salt powder with the desired size. Purchased salt powder with a particle size larger than desired size was crushed and sieved using sieves with the desired mesh. There are two reasons for selecting salt as a space maker. First, it dissolves easily in water, and second, it is hard and does not break at high pressure, and also allows high pressure to be applied in the Micro Die on the powder and acts as a fine die, causing the powder to be more compacted on its surface. Fig. 1 shows the flowchart of the metal foam production process.

According to the results obtained from the optimized stage, the raw materials were weighed with a scale with an accuracy of 0.001 g. The powders were then poured into the mill chamber with powder to ball ratio of 1–4.

The mixer consists of two chambers with a nominal capacity of 12–500 g. The powders were mixed with 3 zirconia pellets at 100 rpm for 1 h.

The ratios of the NaCl and aluminum powder were determined by the final sample volume ($\pi \times r^2 \times h$). The radius and height of the cylinder were equal to r and h, respectively. The amount of volume was calculated according to the Ω and multiplied by the volumetric mass of aluminum (2.7 g/cm^3) and salt (2.16 g/cm^3) to obtain the mass.

For example, for Ω 80% and with a thickness of 1 cm and a diameter of 3 cm, a volume of 7 cm^3 is obtained, that 20% of this volume is 1.4 cm^3 of aluminum with a mass density of 2.7 g/cm^3. By multiplying the volume of aluminum by its mass density, the amount of aluminum is 3.78 g. The amount of salt was also calculated in the same way.

To place the mixed materials inside the SPS, it is necessary to first prepare these mixed materials in the form of pellets. A graphite die (with inner diameter of 30 mm) was used for this purpose. The material of the mentioned die and its mandrel is made of graphite with code R4340 (the SGL company in Germany).

Graphite foil was used to separate the substrate and powder mixture from other die components and to prevent the die from reacting with the powder. For this purpose, each time the inner surface of the die was covered with graphite foil with a thickness of 1 mm.

Then a mixed sample of salt and aluminum powder was placed in the die. A graphite foil and then graphite-circular shape plates were placed on the sample. The graphite die was then mounted on a graphite punch. To prevent heat loss and also overheating of the vacuum chamber, the external environment of the graphite die was covered with a heat-insulating graphite blanket. The graphite die was then placed on the lower electrode with a graphite punch and blanket. Then a graphite pin and a top punch were placed on the die. By applying the appropriate pressure, the upper electrode was connected to the upper punch.

SPS, used in this research, is produced by Easy Fashion metal products trade co. of China. This device has several different parts that include an electric current generator, cooling system, vacuum chamber, vacuum pump, an electric current control system, voltage, pressure and vacuum.

In the continuation of the process, the combination of graphite die and sample was placed inside the steel chamber and then, to measure the temperature, the thermocouple inside the pore was set on the die. Then the top mandrel of the device was placed on the die. After closing the vacuum chamber lid, the vacuum pump was switched on and the air inside the chamber was evacuated (Torr 10^{-2}). One of the advantages of creating a vacuum, in addition to prevent the sample from oxidizing, is the absence of air in the sample to ensure that the Ω of the sample is obtained only from salt.

Then the desired pressure step was set for the sample. To adjust the pressure, first before applying current or heating the sample, a pressure of 10 MPa was applied to the sample and in the next step, after the sample temperature reached a maximum of 420 °C, the final pressure (20 MPa) was applied to the sample [26]. After evacuating the air inside the chamber and reaching a pressure of 10 MPa, an electric current was applied. Pulsed direct electric current was performed with an electric flux or current density of 7 amps per square millimeter. The increase in temperature was accompanied by a gradual increase in electric current at a rate of 8 °C per minute until the aluminum particles were completely sintered [26]. Sintering conditions were selected according to the references, but because the template device model was different from the reference articles, no answer was obtained and as a result, the optimal conditions for this type of sample were obtained by trying and error [24,26,27].

After applying the final pressure and temperature, during the cooling of the sample, first, the mechanical pressure was removed from the sample, then the electric current was reduced. In order to prevent heat cracking and eventual failure of the part, the sample was cooled in a controlled manner. After the temperature of the die and the sample inside it reached ambient temperature, the sample was removed from the die. Fig. 2 demonstrates the sample before (a) and after (b) of the SPS process. In order to perform any analysis, it was first necessary to clean the graphite coating adhering to the sample surfaces by polishing.

After the SPS process was completed and the samples were cooled, the parts were removed from the die and polished to remove graphite foil. This operation was performed first using diamonds and then using sandpaper. Sub-machine and sandpaper of grades 800 and 1000 were used for polishing the polished samples. Therefore, the external surfaces of the sample were free of any contamination and graphite foils.

Finally, to dissolve the salt particles, each sample was first heated separately in a 100 °C water chamber for 180 min. To further

Table 1
Specifications of raw materials.

Row	Material Name	Chemical formula	Purity percentage (%)	Product code	Manufacturer specifications	Country of manufacture
1	Aluminum	Al	99 <	101056	Merck	Germany
2	Salt	NaCl	99.5<	106404	Merck	Germany

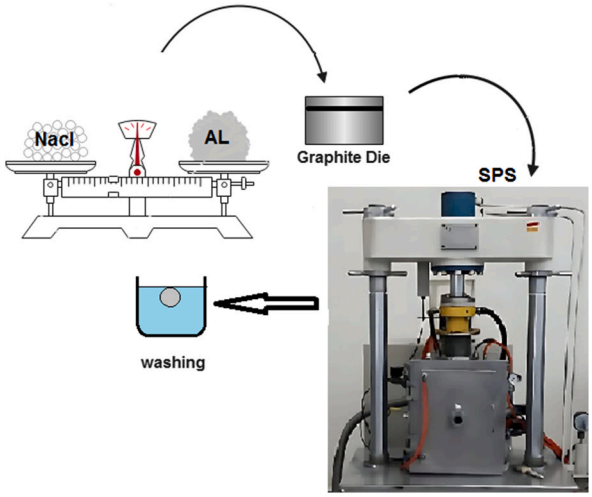

Fig. 1. Flowchart of the process of making metal foam.

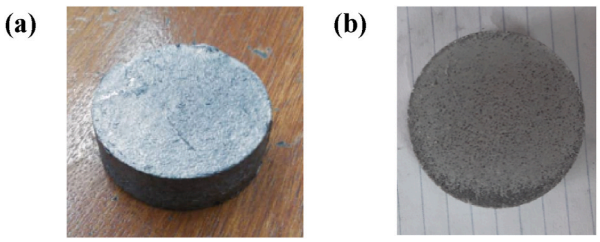

Fig. 2. Sample before (a) and after (b) of the SPS process.

ensure the dissolution of the salt particles, the samples were immersed in water at room temperature for another week. The dissolution steps of the salt are shown in Fig. 3 (Steps1-8). These shapes are taken at 1-day intervals. The floating of the foam in the water indicates the gradual dissolution of the salt in the pores. Finally, by measuring the Ω, all the salt was dissolved in water. Also, according to the different incisions made in the sample to measure the size of the pore with the SEM device, attention was paid to the complete dissolution of the salt.

Ultrasonic Sharper TEK XP-Pro ultrasonic device was used for 10 min to completely dissolve the salt and clean the pores from any contaminants. The power of this device is 120 V and with a frequency of 40,000 Hz.

To determine the density and Ω of the produced foams, first their weight was determined with a digital scale with an accuracy of 0.001 g. Then, according to their regular shape, the volume of each was calculated based on measuring its geometric dimensions.

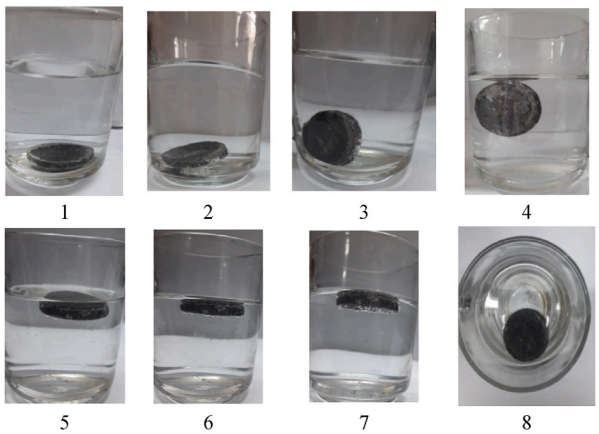

Fig. 3. Steps of dissolving salt in metal foam in water.

Finally, the density of metal foams produced was estimated based on Equation (1). Foam porosities were determined according to ASTM C830-00 [28]. The Ω of each was calculated using the density of aluminum and the density obtained for each of the foams from Equation (2) [8,29].

$$\rho_f = \frac{m}{v} \tag{1}$$

$$\Omega = \left(1 - \frac{\rho_f}{\rho_s}\right) \tag{2}$$

In the above equations m is mass, v is volume, Ω is porosity, ρ_f is the apparent density of the foam and ρ_s is the density of pure aluminum. The density of aluminum is 2.7 g/cm^3 and the density of salt is 2.16 g/cm^3 [30].

Scanning Electron Microscope (SEM) analysis was used to investigate the morphology of spherical pores in the samples [31,32]. The electron microscope used in the present study was the XL30, which operated at a voltage of 30 kV. This device is made by Philips Company in the Netherlands. To analyze the pore structure, the fracture surface from multiple areas was tested. Image Analysis Using ImageJ® software, microstructural features such as D are determined for each foam sample and their average was estimated. During the imaging, because the synthesized samples are conductive, there was no need to use the gold coating on the samples.

2.3. Sound absorption coefficient (SAC) measurement

In this study, to measure the SAC of materials, the SW477 impedance tube of BSWA TECH Company made in China was used (the inner diameter of the test tube is 30 mm). In this experimental study, the SAC of metal foams was measured based on the Transfer Function Method by ISO 10534 standard [33,34]. This was done with the help of a pure sound generator and a calibrated sound level meter. Thus, the SAC of the synthesized samples were measured and examined.

The acoustic tubes consist of an integrated asbestos cylinder with a speaker at one end. The speaker is connected to a pure sound generator and an amplifier. The transfer function method is performed by generating a plate wave in the tube using a speaker and the sound pressure is measured in two moments adjacent to the sample. The acoustic transmission function of two microphone waves is determined and then used to calculate the reflection factor, SAC and impedance ratio of the test materials.

Before testing the materials, the impedance tube was calibrated using the foam sample provided by the device manufacturer. The device was calibrated using the BSWA CA115 model calibrator. Laboratory background noise was measured with an average value of 35 dB.

In all stages of the experiment, according to Table 2, dry temperature, relative humidity and atmospheric pressure were measured and the average of each was entered as input parameters when calculating the SAC in the software. In this study, it was tried that the environmental conditions (temperature and pressure) of the laboratory be under the standard conditions and also the air characteristics be under the theoretical model.

The accuracy (repeatability) of the impedance tube was confirmed by comparing the obtained diagram with the sound absorption curve provided for the foam (in the calibration certificate).

In addition to measure at an optimized specific frequency, the before and after frequencies were also measured. In the present study, for each measurement mode, each sample was paused for 10 min and each mode was repeated three times. For each sample in each position, six measurement modes were performed by shifting the position of the microphones.

3. Results and Discussion

3.1. Microstructural properties of aluminum metal foam

X-ray diffraction diagrams of these materials are shown in Fig. 4-a and 4-b, respectively.

Aluminum oxide (Al_2O_3) was also detected in the aluminum powder due to pre -oxidizing the surface of aluminum powders. SPS method caused the disintegration of aluminum oxide by applying electric current and high pressure.

One of the most important challenges of the present study is the fabrication of open-pore aluminum foam with a very small pore opening size (d) and to the extent that it is required to SAC by the sintering method. If the temperature and pressure exceed a certain value (420 °C and a pressure of 20 MPa), the sample will melt and if they decrease, no sintering will take place. Repeated aluminum foam with an (d) size of 0.1–0.2 mm was made. It was not possible to make other sizes due to what was mentioned above. Because of the mentioned limitation, the (d) was inevitably the same for all samples and equal to 0.1–2.2 mm. As the value of the (d) size of the pore was limited to the above value, the optimization of the (Ω) and (D) values was performed.

Table 2
Parameters used for experimental measurements and their ranges.

Device parameter	Measuring device	model	value	Accuracy or detection limit
Dry air temperature (^{0}C)	Dry thermometer	GDR No.3.89	23 ^{0}C	±0.2^{0}C
Atmospheric pressure (mmhg)	Barometer	Airflow digital barometer D81	760 mmhg	±1 mmHg
Relative humidity (%)	Sky humidity meter	TGL No.94.8300	50%	±5%

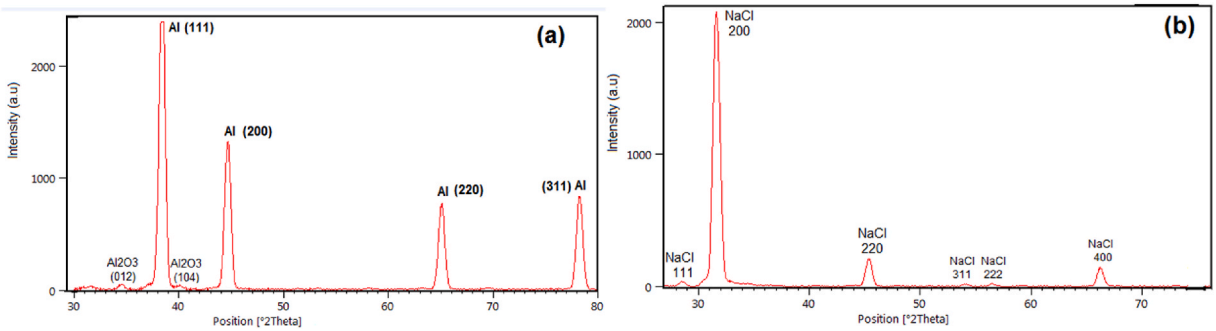

Fig. 4. X-ray diffraction pattern of aluminum powder (a) ans NaCl (b).

After determining the optimal morphological dimensions, the relevant foams were made and their morphological dimensions were determined using SEM imaging (Fig. 5 a: 500 μm and b: 100 μm). The results of optimized (theoretical) and measured (experimental) morphology are shown in Table 3.

To measure the density of the fabric made, first the dimensions of a regular shape of foam were measured with a caliper with accuracy of 0.1 mm and from these dimensions, the volume of the foam was calculated. Then, weight was measured using a digital scale with an accuracy of 0.01 g. Finally, by dividing the weight by the volume, the density of the foam was calculated in the error range of ± 0.03 g/cm^3. To measure the Ω, first, the relative density of the foam relative to the density of the aluminum mass was estimated, then the relative density was subtracted from one and multiplied by 100 (Table 3).

The relative density of the made foams relative to the density of aluminum was also obtained by dividing the density of the foam by the mass density of the material. The approximate amount of aluminum mass density was considered to be 2.7 g/cm^3.

3.2. Measurement of normal incidence sound absorption coefficient

First, the impedance tube device was calibrated. Then, to ensure the correct operation of the device, the standard sample absorption diagram obtained from its manufacturer (BSWA) was compared with the measured absorption diagram of the same sample in the acoustic laboratory. Fig. 6 compares the measured results with the BSWA standard results.

Fig. 6 shows that the measured SAC and the BSWA standard foam values are well matched. The correlation test showed that the measured results had a good correlation with the values of BSWA standard foam (correlation coefficient = 0.99).

After calibrating the impedance tube device, the SAC of foams made in different thicknesses was measured and compared with the values calculated from the Lu model for foam with optimized morphological dimensions. The results of measuring the SAC of optimized aluminum foams for thicknesses of 5, 10, 15 and 20 mm are shown in different frequencies from 1000 to 6300 Hz.

Fig. 7 (a), 8 (a), 9(a) and 10 (a) show the SAC of optimized aluminum foam with a thickness of 5, 10, 15 and 20 mm, respectively.

It is worth mentioning that due to the limited height of the graphite die, it was not possible to make thicker aluminum foam. Optimized peak SAC in thicknesses of 5, 10, 15 and 20 mm were 0.67, 0.9, 1 and 1, respectively. Experimental peak SAC in thicknesses of 5, 10, 15 and 20 mm were 0.44, 0.67, 0.76 and 0.82, respectively. The difference between the optimized (theoretical) SAC and the experimental (measured) at the maximum frequency (maximum SAC) for thicknesses of 5, 10, 15 and 20 were 58%, 33%, 24% and 18%, respectively. Also, the value of the coefficient of determination (COD) (R-Square- R^2) was calculated according to Multiple Linear Regression (MLR). Figs. 7(b) and 8(b), 9(b) and 10(b) demonstrate R-Square (COD) for optimized and experimental SAC. The R-Square

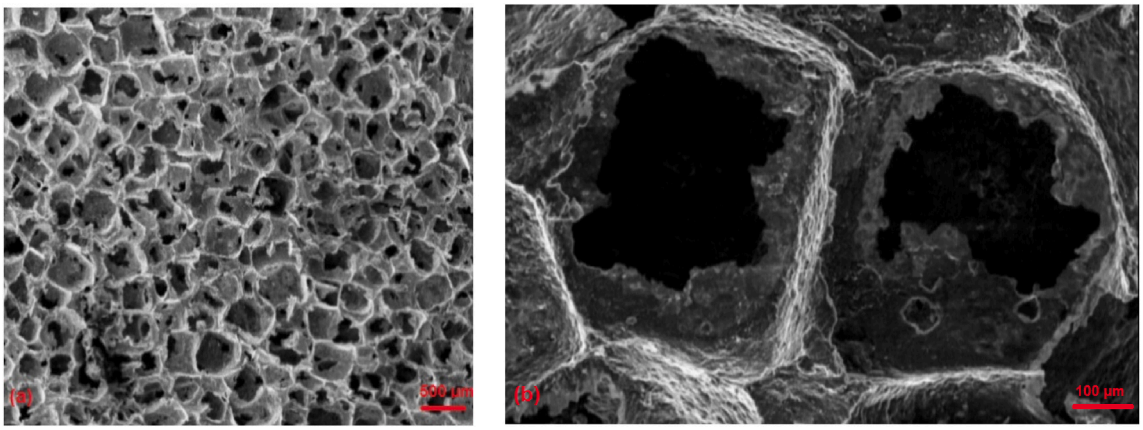

Fig. 5. SEM images of the present aluminium foam sample: at two magnifications.

Table 3
Morphological results of optimized and experimental of aluminum foam.

Row	Sample	Thickness (mm)	Ω (%)	D (mm)	Average d (mm)	Bulk Density (g/m3)	Relative Density
1	Optimized	5	60.21	0.56	0.15	–	–
2	Experimental	5	63.00	0.50–0.65	0.11	1	0.37
3	Optimized	10	80.40	0.54	0.15	–	–
4	Experimental	10	82.00	0.50–0.65	0.14	0.49	0.18
5	Optimized	15	87.54	0.70	0.15	–	–
6	Experimental	15	88.30	0.70–0.88	0.16	0.32	0.11
7	Optimized	20	83.12	0.80	0.15	–	–
8	Experimental	20	85.50	0.70–0.88	0.20	0.4	0.14

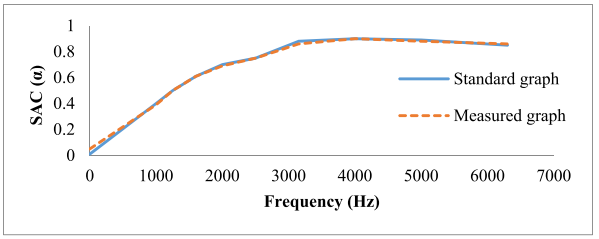

Fig. 6. Comparison values of BSWA standard and measured SAC of thickness 25 mm.

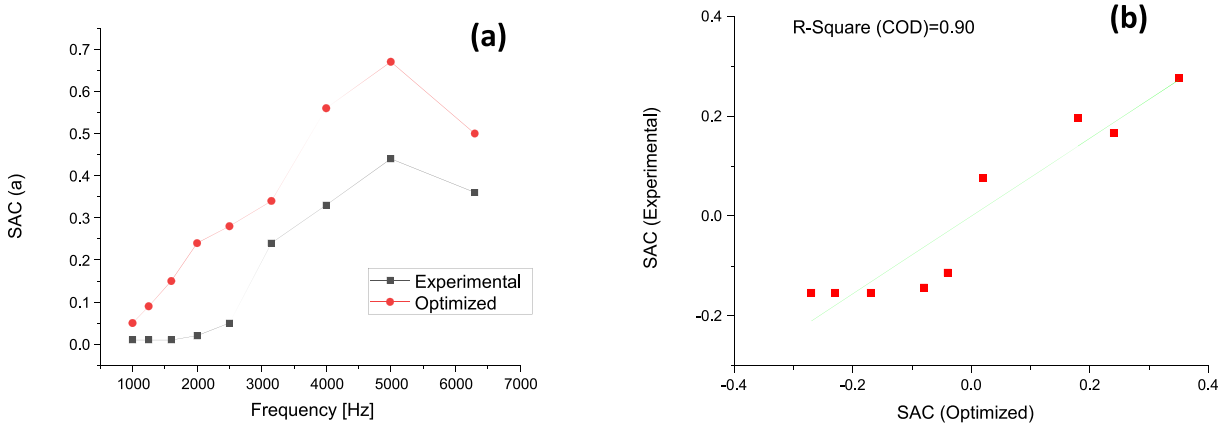

Fig. 7. Optimized and experimental SAC of aluminum foam (5 mm thickness) at different frequencies (a) and R-Square (COD) (b).

(COD) for thicknesses of 5–20 mm was 0.90, 0.95, 0.96 and 0.90, respectively.

In the present study, the porous aluminum foam was prepared by SPS method and then the space particles namely sodium chloride (NaCl) were dissolved by water [35]. In this method, the aluminum powder is sufficiently bonded by SPS, and the thin layer of aluminum oxide cannot prevent the aluminum from sintering. Usually, in other methods such as microwave, this oxide prevents sintering. In addition, by properly mixing the weight ratios and the particle size of the atmosphere (in this study, NaCl), the D, morphology and Ω of the metal foam can be easily controlled.

The mechanism of sound absorption by porous absorbers such as foams is due to the conversion of the energy of sound waves into heat energy due to the movement of these waves in irregular paths within these materials and friction with them, as well as multiple reflections and scattering from walls and edges of foam pores [36,37].

In aluminum foam, by selecting the appropriate thickness, Ω and D, the ideal absorption can be achieved. The flow resistance and structure of the foam can be affected by the pore structure and Ω of the metal foam and ultimately the SAC. In metal foam with a suitable pore structure and Ω, better absorption can be achieved than flexible materials (such as polymers).

In 2018, liang et al. Compared the effect of sound absorption on three foams of copper, nickel and aluminum and concluded that aluminum foam has a better SAC than nickel and copper foam due to its more complex pore structure and rougher wall [38]. Cellular materials are directly attached to the rigid wall mainly SAC through the mechanism of the adhesion effect. The ability to SAC in these cellular materials depends on the flow resistance in the pore structure [39,40]. According to Li et al. study, the matrix in porous materials with rigid frames such as aluminum has less inherent damping than polymeric materials [8]. Therefore, the SAC of a porous

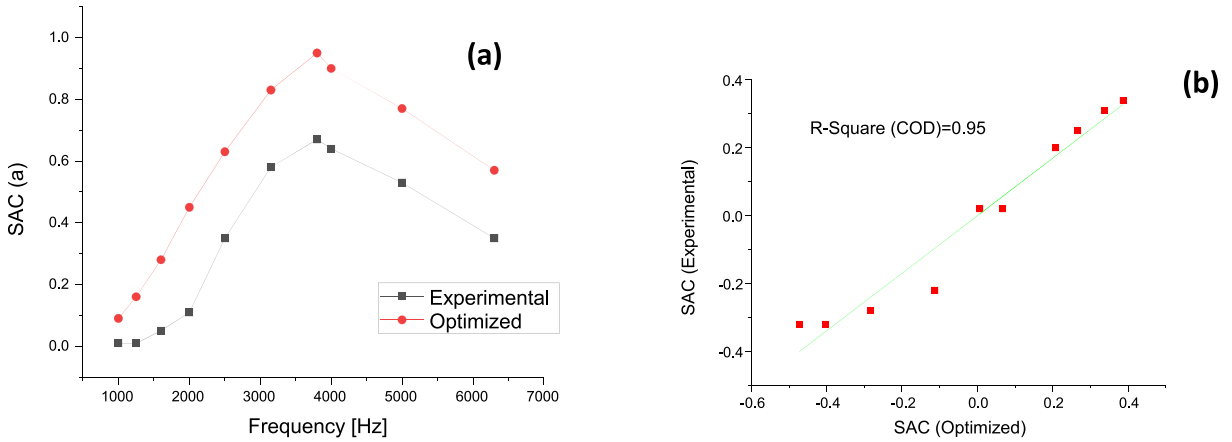

Fig. 8. Optimized and experimental SAC of aluminum foam (10 mm thickness) at different frequencies (a) and R-Square (COD) (b).

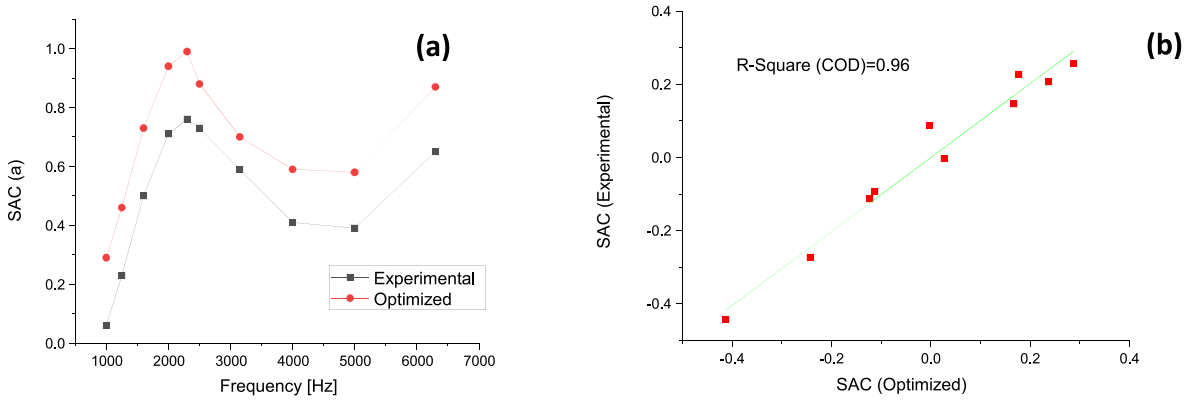

Fig. 9. Optimized and experimental SAC of aluminum foam (15 mm thickness) at different frequencies (a) and R-Square (COD) (b).

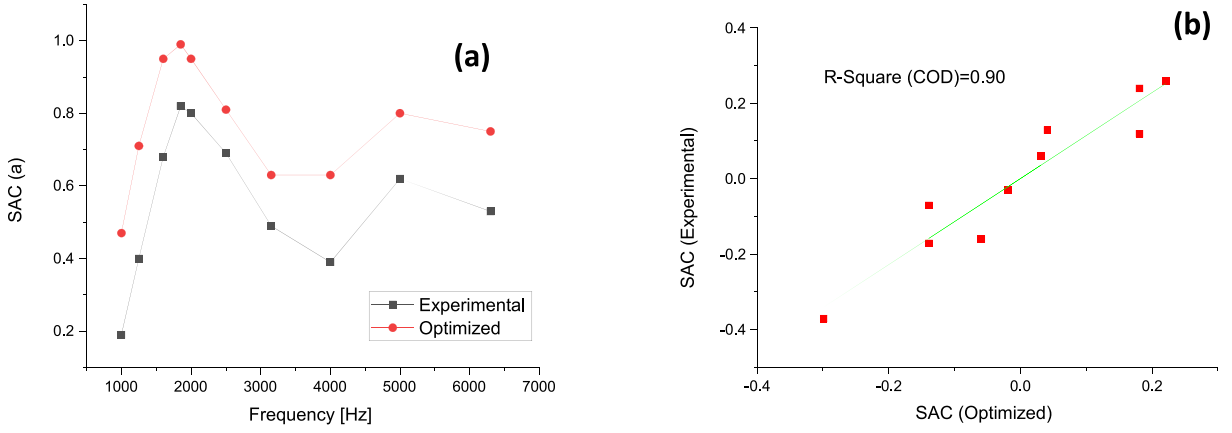

Fig. 10. Optimized and experimental SAC of aluminum foam (20 mm thickness) at different frequencies (a) and R-Square (COD) (b).

material with a rigid frame mainly depends on the structure of the pores, including Ω, as well as the size and connection of the pores(D, d).

In the present study, some limitations, such as the lack of precise control of the (d) size and the thickness of the graphite die during foam fabrication, led to a re-optimization for the (d) size with an average of 0.15 mm. According to the results of re-optimization, metal foam with thicknesses of 5, 10, 15 and 20 mm was made and the frequency optimization range was 2000 Hz, 2500 Hz, 4000 Hz and 5000 Hz, respectively. According to the results of this study, there was a good R-Square (mean $R^2 = 0.92$) between the optimized and

experimental methods, which is an acceptable result. The R-Square (COD) is one of the useful criteria in evaluating some statistical methods.

One of the challenges of accurately controlling the (d) size is the preparation of salt particles of the size obtained by the optimization method. Since the production of salt particles of the same size and size obtained by the optimization method is almost impossible, a slight difference was observed between the experimental and optimized results. Despite this limitation, the frequencies considered for the maximum SAC had a higher SAC than the adjacent frequencies. In this study, for thicknesses of 5 and 10 mm, the optimal (D) range is in the range of 0.5–0.65 mm. In 2000, Lu et al. reported in their research that pore diameters of 0.5 mm were more important in the SAC [11]. In this regard the results of the study of Lu et al. are consistent with the obtained results of the present study [11].

According to the results, it seems that the amount of Ω and morphology of the pore (D, d) at each frequency and thickness have a different value for the maximum SAC, so by optimizing and building them accurately, this can be achieved.

4. Conclusions

In this study, the aluminum foam was optimized, designed and then fabricated to sound absorbing at a certain frequency using a Lu theoretical model. Sampels made by impedance tube device were tested. The summary of the most important results of this study is as follows:

1. Using the SPS can be a suitable method for preparing sound-absorbing metal foam.
2. The two methods of experimental measurement and Lu theoretical model showed good agreement.
3. Optimized and experimental SAC were well matched (mean $R^2 = 0.92$).
4. The sound optimal absorber at each frequency and thickness has a value of the Ω and the (D) size variable for the maximum SAC, which is determined by optimizing their amount.
5. With the approach used in the present study, it is possible to predict the SAC of aluminum foam and adapt it to the needs of acoustic design without the need for costly trial and error methods.

The main limitations of the present study were: 1. Limitation of the thickness of the graphite die of the SPS machine 2. It was difficult to obtain the exact size of the salt according to the optimization results. 3. Precise control of the (d) size of the pore was not possible when making metal foam with a SPS machine.

Author contribution statement

Mohammad Javad Jafari: Conceived and designed the experiments; Analyzed and interpreted the data; Wrote the paper.
Rohollah Fallah Madvari: Conceived and designed the experiments; Performed the experiments; Wrote the paper.
Touraj Ebadzadeh: Analyzed and interpreted the data; Contributed reagents, materials, analysis tools or data; Wrote the paper.

Data availability statement

Data will be made available on request.

Additional information

No additional information is available for this paper.

Declaration of competing interest

The authors have no interests to declare.

Acknowledgement

The authors would like to extend their gratitude and acknowledgments to study team members for their time and energy spent on this project (Ethic code: IR.SBMU.PHNS.REC.1397.103).

References

[1] H. Meng, et al., Sound absorption coefficient optimization of gradient sintered metal fiber felts, Sci. China Technol. Sci. 59 (5) (2016) 699–708.
[2] W. Zhai, et al., Microstructure-based experimental and numerical investigations on the sound absorption property of open-cell metallic foams manufactured by a template replication technique, Mater. Des. 137 (2018) 108–116.
[3] M. Hakamada, et al., High sound absorption of porous aluminum fabricated by spacer method, Appl. Phys. Lett. 88 (25) (2006), 254106.
[4] J. Trevor, P. Dantonio, Acoustic Absorbers and Diffusers, Taylor & Francis, 2009.
[5] S. Boominathan, et al., Influence of fiber blending on thermal and acoustic properties nonwoven material, J. Nat. Fibers 19 (15) (2022) 11193–11203.

[6] M. Bogale, et al., Sound absorbing and thermal insulating properties of recycled cotton/polyester selvedge waste chemical bonded nonwovens, J. Text. Inst. 114 (1) (2023) 134–141.
[7] S. Sakthivel, et al., Recycled cotton/polyester and polypropylene nonwoven hybrid composite materials for house hold applications, J. Text. Inst. 113 (1) (2022) 45–53.
[8] Y. Li, et al., Sound absorption characteristics of aluminum foam with spherical cells, J. Appl. Phys. 110 (11) (2011), 113525.
[9] M. Hakamada, et al., Sound absorption characteristics of porous aluminum fabricated by spacer method, J. Appl. Phys. 100 (11) (2006), 114908.
[10] T. Kuromura, et al., Sound absorption behavior of porous Al produced by spacer method, in: Advanced Materials Research, Trans Tech Publ, 2007.
[11] T.J. Lu, F. Chen, D. He, Sound absorption of cellular metals with semiopen cells, J. Acoust. Soc. Am. 108 (4) (2000) 1697–1709.
[12] M.J. Jafari, et al., Optimization of the morphological parameters of a metal foam for the highest sound absorption coefficient using local search algorithm, Arch. Acoust. Q. 45 (3) (2020) 487–497.
[13] R.F. Madvari, et al., Estimation of Metal Foam Microstructure Parameters for Maximum Sound Absorption Coefficient in Specified Frequency Band Using Particle Swarm Optimisation, Archives of Acoustics, 2022, pp. 33–42, 33-42.
[14] T.F. Gonzalez, Handbook of Approximation Algorithms and Metaheuristics, Chapman and Hall/CRC, 2007.
[15] J. Banhart, Manufacture, characterisation and application of cellular metals and metal foams, Prog. Mater. Sci. 46 (6) (2001) 559–632.
[16] T. Miyoshi, et al., ALPORAS aluminum foam: production process, properties, and applications, Adv. Eng. Mater. 2 (4) (2000) 179–183.
[17] M. Kobashi, N. Kanetake, Processing of intermetallic foam by combustion reaction, Adv. Eng. Mater. 4 (10) (2002) 745–747.
[18] A. Simone, L. Gibson, Efficient structural components using porous metals, Mater. Sci. Eng., A 229 (1–2) (1997) 55–62.
[19] J. Park, et al., Microstructure and mechanical behavior of AISI 4340 steel fabricated via spark plasma sintering and post-heat treatment, Mater. Sci. Eng., A 862 (2023), 144433.
[20] M. Tokita, Progress of spark plasma sintering (SPS) method, systems, ceramics applications and industrialization, Ceramics 4 (2) (2021) 160–198.
[21] N. Sharma, S. Alam, B. Ray, Fundamentals of spark plasma sintering (SPS): an ideal processing technique for fabrication of metal matrix nanocomposites, Spark plasma sintering of materials: advances in processing and applications (2019) 21–59.
[22] A.T. Rosenberger, Sintering Techniques for Microstructure Control in Ceramics, Purdue University, 2015.
[23] C. Wen, et al., Processing of fine-grained aluminum foam by spark plasma sintering, J. Mater. Sci. Lett. 22 (20) (2003) 1407–1409.
[24] M. Hakamada, et al., Effect of sintering temperature on compressive properties of porous aluminum produced by spark plasma sintering, Mater. Trans. 46 (2) (2005) 186–188.
[25] M.-J. Jafari, et al., Improving the morphological parameters of aluminum foam for maximum sound absorption coefficient using genetic algorithm, Sound \& Vibration 55 (2) (2021) 117–130.
[26] D.V. Dudina, B.B. Bokhonov, E.A. Olevsky, Fabrication of porous materials by spark plasma sintering: a review, Materials 12 (3) (2019) 541.
[27] M. Hakamada, et al., Compressive properties at elevated temperatures of porous aluminum processed by the spacer method, Journal of materials research 20 (12) (2005) 3385–3390.
[28] ASTM C830-00, Standard Test Methods for Apparent Porosity, L.A., Apparent Specific Gravity, and Bulk Density of Refractory Shapes by Vacuum Pressure, American Society for Testing and Materials, West Conshohocken, PA, USA, 2010.
[29] H. Ke, et al., Acoustic absorption properties of open-cell Al alloy foams with graded pore size, Journal of Physics D: Applied Physics 44 (36) (2011), 365405.
[30] A. Brothers, D. Prine, D.C. Dunand, Acoustic emissions analysis of damage in amorphous and crystalline metal foams, Intermetallics 14 (8–9) (2006) 857–865.
[31] W. Zhou, Z.L. Wang, Scanning Microscopy for Nanotechnology: Techniques and Applications, Springer science & business media, 2007.
[32] N. Babcsán, et al., The role of oxidation in blowing particle-stabilised aluminium foams, Advanced Engineering Materials 6 (6) (2004) 421–428.
[33] E. Iso, 10534-2: 2001 Acoustics—Determination of Sound Absorption Coefficient and Impedance in Impedances Tubes—Part 2: Transfer-Function Method, ISO, Brussels, Belgium, 2001 *(ISO 10534-2: 1996)*.
[34] I.S. Iso, 10534-1," Acousticsdetermination of Sound Absorption Coefficient and Impedance in Impedance Tubes-Part 1: Method Using Standing Wave Ratio", International Standard, 1996.
[35] C. Wen, et al., Processing of fine-grained aluminum foam by spark plasma sintering, Journal of materials science letters 22 (1407–1409) (2003) 1407–1409.
[36] L.L. Beranek, I.L. Ver, *Noise and Vibration Control Engineering-Principles and Applications.* Noise and Vibration Control Engineering-Principles and Applications, John Wiley & Sons, Inc., 1992, p. 814.
[37] M. Möser, Engineering Acoustics: an Introduction to Noise Control, Springer Science & Business Media, 2009.
[38] L.S. Liang, et al., The sound absorption properties comparison of metal foams and flexible cellular materials, in: Materials Science Forum, Trans Tech Publ, 2018.
[39] M. Nosko, et al., Sound absorption ability of aluminium foams, Metallic foams 1 (1) (2017) 15–41.
[40] C. Guiping, H. Deping, S. Guangji, Underwater sound absorption property of porous aluminum, Colloids and Surfaces A: Physicochemical and Engineering Aspects 179 (2–3) (2001) 191–194.